We are IntechOpen, the world's leading publisher of Open Access books
Built by scientists, for scientists

6,900
Open access books available

185,000
International authors and editors

200M
Downloads

154
Countries delivered to

Our authors are among the

TOP 1%
most cited scientists

12.2%
Contributors from top 500 universities

CLARIVATE ANALYTICS
BOOK CITATION INDEX
INDEXED

WEB OF SCIENCE™

Selection of our books indexed in the Book Citation Index
in Web of Science™ Core Collection (BKCI)

Interested in publishing with us?
Contact book.department@intechopen.com

Numbers displayed above are based on latest data collected.
For more information visit www.intechopen.com

Engineering Nanostructured MnO$_2$ for High Performance Supercapacitors

Jian-Gan Wang

Additional information is available at the end of the chapter

Abstract

Manganese oxides (MnO$_2$) have particularly received increasing attention owing to their high theoretical specific capacitance of 1370 F/g, low-cost, natural abundance, and environmental benignity. However, MnO$_2$ suffers from low electrical conductivity (10^{-5} to 10^{-6} S/cm), low ionic diffusion constant ($\sim 10^{-13}$ cm^2/V s), and low structural stability, which results in low electrochemical utilization and poor cycling life. It is therefore important to explore new strategies to improve the electrochemical performance of MnO$_2$. The effective methods to maximize the performance involve (i) reducing MnO$_2$ structures to a nanoscale range and (ii) compositing MnO$_2$ with highly conductive materials. In this chapter, we will first introduce the rapid development of MnO$_2$ nanostructures for supercapacitors. Then the fundamental charge storage mechanism of MnO$_2$ will be specifically clarified. The preparation methods of MnO$_2$ nanostructures and their composites will be subsequently summarized. Then, we will pay great attention to the most recent development of MnO$_2$-based nanostructures for supercapacitors, which is the main body of this chapter. The practical application of MnO$_2$ nanostructures for symmetric and asymmetric supercapacitors will be discussed. Finally, we will present a brief perspective regarding the rational design and synthesis of MnO$_2$-based nanostructures.

Keywords: MnO$_2$, nanostructure, composite, supercapacitor, high performance

1. Introduction

According to the charge storage mechanism, supercapacitors can be categorized as electrochemical double layer capacitors (EDLCs) and pseudocapacitors [1]. The typical electroactive electrode materials for pseudocapacitors include transition-metal oxides and conducting

polymers. To this end, massive efforts have been dedicated to developing low-cost and eco-friendly alternatives, such as MnO_2, Co_3O_4, and NiO. Among the alternative candidates, MnO_2 has received intensive attention in the past decades. Lee and Goodenough reported the first use of MnO_2 for supercapacitors in 1999 [2]. This finding paved a new avenue for exploring a huge variety of electroactive MnO_2-based electrode materials for high performance super-capacitors. This is because MnO_2 shows advantages of (i) a high theoretical specific capacitance of 1370 F/g; (ii) a wide operating potential window of about 1.0 V; and (iii) the ability to enable mild aqueous electrolytes with a much less chemical corrosion to current collectors or packages [3, 4]. In addition, MnO_2 has additional merits of natural abundance, low-cost, and environmentally benignity [4]. These unique characteristics will enable MnO_2-based electrodes to act as a high-performance, safe, and a low-cost replacement.

However, the specific capacitance of MnO_2 is almost one magnitude lower than the theoretical value [4–6]. This is because MnO_2 shows poor electronic conductivity (10^{-5} to 10^{-6} S/cm), low ionic diffusion constant (~10^{-13} cm^2/V s), and structure flexibility [7, 8]. Moreover, owing to a wide diversity of textural feature, crystal forms (e.g., α-, β-, δ-, γ-MnO_2), and defect chemistry, MnO_2 exhibits a variety of distinct electrochemical performance. The performance of MnO_2 will be substantially improved with a better fundamental understanding of the charge storage mechanism at the electrode/electrolyte interfaces and a rational design of MnO_2-based electrodes.

In recent years, extensive endeavors have been dedicated to synthesizing MnO_2 nanostructures or nanocomposites with different morphologies and crystal forms. This chapter will introduce the state-of-the-art MnO_2 electrodes for high performance supercapacitors. The content includes a brief discussion of the charge storage mechanisms of MnO_2, a summary of the synthetic methodologies, a main focus on the MnO_2-based electrodes and their application in supercapacitors.

2. Charge storage mechanism of MnO_2

The charge storage mechanism of MnO_2 was first imitated from RuO_2 and Zn/MnO_2 cells in acidic electrolytes [9], which involve a reversible insertion/extraction of protons into/from MnO_2 with a concomitant Mn^{3+}–Mn^{4+} transition. However, the specific capacitance of MnO_2 is found to be related to the species and concentrations of the alkali metal cations, such as Li^+, Na^+, and K^+, regardless of the pH value [10, 11]. Consequently, a more rational mechanism based on the chemisorption of alkali metal cations on the surface of MnO_2 was proposed and can be written as [3, 11]:

$$\left(MnO_2\right)_{surface} + M^+ + e^- \rightarrow \left(MnOOM\right)_{surface} \tag{1}$$
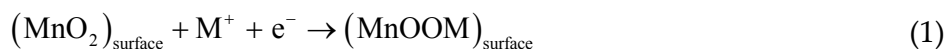
where M^+ represents alkali metal cations, including Li^+, Na^+, and K^+. Later, Belanger and co-workers developed a new complementary storage mechanism, that is, the alkali metal cations can insert/extract into/from MnO_2, as shown in Eq. (2) [11]:

$$MnO_2 + M^+ + e^- \rightarrow MnOOM \tag{2}$$

It should be noted that MnO$_2$ can crystallize in various forms. Can the above charge storage mechanisms be suitable for all MnO$_2$ structures? Brousse et al. investigated a systematic comparison on the supercapacitive properties of MnO$_2$ with five types of phase structures [11]. It is revealed that the capacitance is closely associated with the tunnel size of crystalline MnO$_2$, i.e., the larger the tunnel size, the larger the specific capacitance. More specifically, the one-dimensional (1D) α-MnO$_2$ (4.6 Å) and two-dimensional (2D) δ-MnO$_2$ (7 Å) allow a fast insertion of hydrated K$^+$ cations (3 Å) due to their large tunnel sizes, while β-MnO$_2$ and γ-MnO$_2$ with one-dimensional tunnel sizes smaller than cations limit the diffusion process, and the spinel λ-MnO$_2$ with a more opened three-dimensional (3D) structure can permit a partial cationic diffusion. This suggests that the tunnel space should be large enough to allow a high-rate insertion/extraction of electrolyte ions for charge storage governed by Eq. (2), which is known as "tunnel storage mechanism (TSM)" [12]. Hence, the specific capacitance of MnO$_2$ depends strongly on its crystallographic structure, which follows the decreasing order: $\alpha(m) > \alpha \approx \delta > \gamma > \lambda > \beta$. Furthermore, owing to the large tunnel, α-MnO$_2$ also exhibits ideal pseudocapacitive behavior in the electrolytes containing Ca^{2+}, Mg^{2+}, or Ba^{2+}, which can store more charge through a multivalent cation storage mechanism [5]. In addition to the metal cations, anions can also be the working species that compensate the Mn-valent state variation upon charge/discharge in aprotic ionic liquids (IL) [13]. In summary, the charge/discharge process of MnO$_2$ typically involves (i) electrolyte ion transport; (ii) ion adsorption/desorption at the surface sites of electrodes, which are dependent on the ion size, the mobility of ion, and the dehydration/hydration rate; and (iii) ion insertion/extraction into/from bulk MnO$_2$. Therefore, the charge storage process is not only associated with crystallographic structures, but also relates to other factors, such as specific surface area, electronic conductivity, and ionic conductivity, etc. Therefore, the charge storage mechanism of MnO$_2$ basically involves a capacitive surface chemisorption process (Eq. (1)) and a bulk/subsurface Faradaic reaction (Eq. (2)).

Recently, mixed-valent chemistry of metal oxides charge compensation mechanisms at oxygen centers and surfaces were proposed as a new charge storage mechanism. The mixed-valent MnO$_x$ nanostructures exhibited a high-specific capacitance of 2530 F/g in a two-electrode configuration, about double of the theoretical value (1370 F/g) [14]. It is revealed that a large portion of charge compensation might be originated from the hole state redistribution toward the O sites, rather than merely reduction of Mn ions. In addition, the ionic defects (vacancies and misplaced ions), electronic defects (electron and holes), and structural defects (cavities, stacking faults, etc.) in the mixed-valent MnO$_x$ can also boost the kinetics of the surface redox reactions and the transport of charged species. These findings may offer critical insights into the fundamental understanding of the relationship between mixed-valent structures and electrochemical properties and to rational design of a new-generation supercapacitors.

3. Synthesis methods

3.1. Chemical precipitation

MnO_2 nanostructures can be easily prepared *via* various chemical co-precipitation methods. The most commonly one is based on a simple redox reaction between MnO_4^- and Mn^{2+} [4]:

$$2MnO_4^- + 3Mn^{2+} + 2H_2O \rightarrow 5MnO_2 + 4H^+ \tag{3}$$
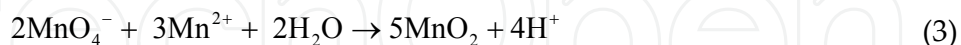
Amorphous hydrated MnO_2 powders are the resulting products at room temperature. Increasing the reaction temperature not only leads to an increase in the degree of MnO_2 crystallinity, but also generates different morphologies, such as nanorods, nanoflowers, and nanotubes [15]. Because of the strong oxidation of MnO_4^-, a large number of reducing species, including acid, polymer monomers, carbon, etc., can be used to obtaining MnO_2 nanostructures [16]. In addition, MnO_2 can also be gained by changing other oxidants, such as $Na_2S_2O_8$, $KClO_3$, etc. These flexible derived reactions facilitate the formation of MnO_2-carbon and MnO_2-conducting polymer nanocomposites [17].

3.2. Electrodeposition

3.2.1. Anodic electrodeposition

Anodic electrodeposition of MnO_2 nanostructures involves an oriented diffusion of Mn^{2+} species to the anode surface under an applied electric field and a subsequent electro-oxidation of the species into MnO_2. The anodic deposition reaction can be expressed as [18]:

$$Mn^{2+} + 2H_2O \rightarrow MnO_2 + 4H^+ + 2e^- \tag{4}$$
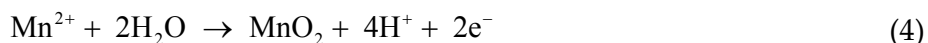
Three different deposition techniques have been developed: i.e., potentiostatic deposition, potentiodynamic deposition, and galvanostatic deposition. The morphology can be well controlled by modifying the deposition parameters (such as applied potentials, applied currents, scan rates, electrolyte ingredients/concentrations, and pH value, etc.) and by tuning the physiochemical nature of substrates (such as a porous structure, a hydrophilic surface, etc.).

In addition to pure MnO_2, conducting polymer-MnO_2 nanocomposites can also be fabricated using solution precursors containing both Mn^{2+} species and monomers [19]. One-step or two-step electrochemical co-deposition has been explored to effectively prepare a nanocomposite. The co-electrodeposition process primarily involves the anodic deposition of MnO_2 and the simultaneous electropolymerization of conducting polymers. The morphology of the nano-structured hybrids can be controlled by modifying the deposition parameters.

3.2.2. Cathodic electrodeposition

Cathodic electrodeposition of MnO$_2$ nanostructures can take place at the cathode surface *via* two pathways based on Mn species in solution under a negative potential. The first way is based on the electrochemical processes in aqueous solution containing Mn^{2+} species, which include water electrolysis and oxygen reduction to generate OH$^-$, followed by the precipitation of metastable Mn(OH)$_2$ and a further oxidation into MnO$_2$. The other pathway is on basis of the reduction of Mn^{7+} species from MnO$_4^-$ on the cathode surface, following reaction (5) [20]. The MnO$_2$ nanostructures can be shape-controlled by tuning deposition variables of current density, potential, solution concentration, and pH value.

$$MnO_4^- + 2H_2O + 3e^- \rightarrow MnO_2 + 4OH^- \tag{5}$$

3.3. Electrostatic interaction assembly

Electrostatic interaction assembly is an effective technique for fabricating nanocomposites *via* a self-assembly of oppositely charged materials. The strong electrostatic attractive interactions between positively charged species and negatively charged species can ensure the robustness of resulting materials. The binding intensity of the electric force is determined by the Coulomb's law [21]:

$$F = q_+ q_- / r^2 \tag{6}$$

where F is the electric force, q_+ and q_- are the charges of the negative and positive species, and r is the distance between the two species. The main challenge is to controllably modify the target material surfaces with negatively/positively charged species, such as negatively charged poly(styrene sulfonate) (PSS), and positively charged aminopropyltrimethoxysilane (APTS) moieties and poly(diallyldimethylammonium chloride) (PDDA) [22].

4. Electrochemical performance of pure MnO$_2$ nanostructures

4.1. Amorphous MnO$_2$ powder electrodes

The MnO$_2$ powders prepared at low temperatures are generally amorphous or poorly crystalline in nature [23]. In addition, the as-prepared samples often contain a certain amount of hydrated content, which exists in the form of residual structural water and/or hydrated trivalent MnOOH. The hydrated MnO$_2$ powders have large surface area because of ultrafine nanoparticle morphology. Although the amorphous structure can be maintained up to 300°C, the hydrated amount and the surface area decrease significantly with increasing annealing temperature and dwelling time [8, 24].

The electrochemical properties of the amorphous MnO_2 powder electrode are closely related to their surface area and hydrated amount. According to the Eq. (1), an increase in the surface area is rather favorable for enhancing specific capacitance. The hydrated species can also modify the MnO_2 surface affinity, which facilitates the electrolyte access and ion transport for enhanced performance. It was revealed that the amorphous MnO_2 had the largest surface area and also possessed the best electrochemical performance. A dramatic decrease in the surface area and water content were observed after annealing treatments, which, in turn, degraded the specific capacitance.

4.2. Crystalline MnO_2 powder electrodes

As mentioned earlier, MnO_2 can exist in various crystal forms. The arrangement of $[MnO_6]$ basic building unit enables the construction of one-dimensional, two-dimensional, and three-dimensional tunnel structures. The tunnel space, depending on the tunnel sizes, can accommodate cations, such as K^+, Na^+, Li^+, Ca^+, Mg^+, etc., which favors the energy storage according to Eq. (2). Recently, Ghodbane et al. has carried out a systematic study dealing with the microstructural effects on electrochemical properties in crystalline MnO_2 [7]. As shown in **Figure 1**, the three-dimensional spinel λ-MnO_2 exhibits the highest specific capacitance followed by the two-dimensional δ-MnO_2 and, finally, the one-dimensional group shows the lowest values. To some extent, the specific capacitance increases with an increase in the tunnel size. One exception is the Ni-todorokite, which has a large tunnel size but a low-specific capacitance. The reason is the presence of very short and strong hydrogen bonds, which stabilize the hydrated cations inside the cavity and impede the ion diffusion through the tunnels. Additionally, it was found the specific capacitance did not depend on the specific surface area, and the ionic conductivity exerted great influence on the electrochemical performance. The comparison suggests the charge storage in MnO_2 is a fundamentally Faradaic process.
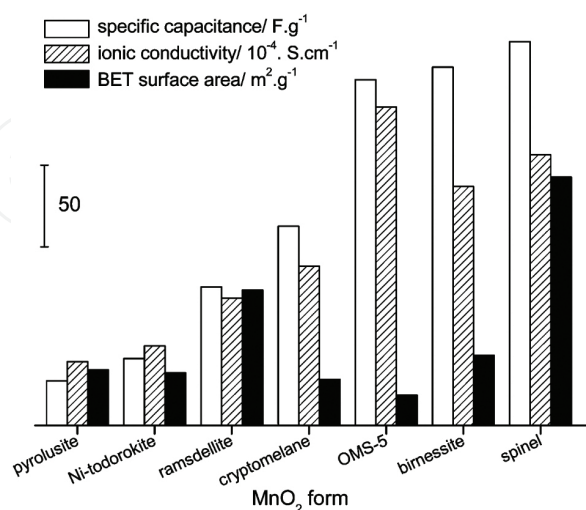

Figure 1. Comparison of the specific capacitance, ionic conductivity, and surface area of various MnO_2 nanostructures [7].

Hydrothermal or solvothermal methods are appropriate techniques to prepare MnO$_2$ nanostructures, including nanorods, nanotubes, and nanowires, [4, 15]. The as-prepared products showed distinct morphologies, but the electrochemical results are highly scattered. There is no consistent relationship among the synthesis conditions, microstructures, and specific capacitance. In general, MnO$_2$ with high crystallinity shows a low-specific surface area, and the cations in the tunnel structure are difficult to be extracted for TSM, thereby resulting in limited specific capacitance.

4.3. Thin-film MnO$_2$ electrodes

Thin-film MnO$_2$ electrodes have been massively explored for deepening fundamental studies and finding potential applications as microscale energy storage devices. In this regard, a number of MnO$_2$ thin-film electrodes have been directly prepared on a current collector, such as metal foils, carbon cloth, etc., through anodic/cathodic electrodeposition. In terms of the charge storage mechanism, the most desirable morphology should be of three-dimensional and porous nanoarchitectures with good connection to a highly conductive substrate. Therefore, much effort has focused on the morphology-controlled growth of porous MnO$_2$ nanostructures, with a purpose of obtaining more accessible electroactive sites and short ion diffusion pathways. This can be achieved by controlling the deposition conditions and using porous templates. For example, galvanostatic, or potentiostatic techniques were employed to fabricate porous fibrous network, nanorods, and nanosheets [25–27].

As for anodic electrodeposition, chemically stable metal (e.g., Ti or Ta foils, etc.) and carbon (graphites, carbon fabric, etc.) substrates should be employed to address the problem of anodic oxidation and dissolution of metal substrates (e.g., stainless steel). In sharp contrast, cathodic deposition is a good method to break this limit. Electrodeposition from a dilute NaMnO$_4^-$ solution (0.02 M) produced a typical surface morphology of fibrous film with a birnessite-type crystal structure [28]. Compared to the pure MnO$_2$ powders in Sections 4.1 and 4.2, the MnO$_2$ thin films can deliver much higher specific capacitance.

4.4. Summary

Pure MnO$_2$ nanostructures with different crystal phases and morphologies can be easily prepared using solution-based methods. Unfortunately, the overall specific capacitances of the amorphous and crystalline MnO$_2$ powders are mostly ranging from 100 to 250 F/g, which are far from satisfaction. According to the charge storage mechanisms, the Faradaic reactions of MnO$_2$ only occur at the surface or subsurface within tens of nanometers. Thus, to maximize the high electrochemical utilization of MnO$_2$, the thickness of MnO$_2$ should be kept in a nanoscale range. This is confirmed by a high-specific capacitance of 300–800 F/g when MnO$_2$ thin films were deposited on the conductive substrates. The specific capacitance can even reach the theoretical value when thickness of MnO$_2$ film is only several nanometers. The reason can be rationalized by the nanostructured MnO$_2$ shortening both ionic and electronic transport/diffusion distances for faster reaction kinetics. However, the thin films are limited by their low mass loading, which cannot meet large scale practical applications.

5. Electrochemical performance of MnO$_2$-based nanocomposites

5.1. MnO$_2$-carbon nanocomposites

Over the past decades, carbon nanostructures have received intensive attention in various communities of material science and chemistry. First, carbon nanostructures are the most effective electrode material candidates for EDLCs owing to the versatile size dimensionality, high surface area, good electrical conductivity, and strong structural stability. Nevertheless, carbon-based electrodes are limited by their low specific capacitance. To break this limitation, carbon structures often serve as favorable supports for MnO$_2$ by making complementary functions. In this section, we emphasize on the composites with one-dimensional carbon nanotubes (CNTs) two-dimensional, graphene, and three-dimensional mesoporous carbon [29].

5.1.1. MnO$_2$-CNTs

CNTs exhibit fascinating physicochemical properties of high electrical conductivity, high surface area, good chemical stability, and strong mechanical strength [29]. CNTs are increasingly employed as substrates for anchoring pseudocapacitive MnO$_2$, to form nanocomposites. The nanocomposites can utilize the large pseudocapacitance of MnO$_2$ and the conducting and mechanical merits from CNTs. Moreover, the nanocomposites could inherit the well-developed CNTs networks with open mesopores. Consequently, the MnO$_2$-CNTs nanocomposites are expected to exhibit superior electrochemical properties. The key issue to obtain high-performance MnO$_2$/CNT nanocomposites is how to uniformly deposit nanostructured MnO$_2$ onto CNTs. To ensure the uniformity, the CNT powders should be homogeneously dispersed in a solution by means of surface modification and/or ultrasonic treatments. The three-dimensional CNT network in the suspension can combine MnO$_2$ nanostructures (e.g., nanorods or nanoclusters) using various chemical or electrochemical deposition methods. The most favorable method is based on a spontaneously redox reaction of MnO$_4^-$ and carbon, enabling *in situ* deposition of MnO$_2$ on CNTs [30–32]. **Figure 2a** shows a typical core-sheath hierarchy architecture constructing by MnO$_2$ nanostructures surrounding the CNT surfaces [33]. Under assistances of some modified techniques, such as the hydrothermal method, the refluxing, and the microwave irradiation, a variety of MnO$_2$/CNT nanocomposites with different mass loadings and morphologies (e.g., nanoflakes and nanorods) of MnO$_2$ have been demonstrated to exhibit improved electrochemical performance.

In addition to the surface deposition, MnO$_2$ nanoparticles can also be embedded into the well-defined CNT nanochannels, as shown in **Figure 2b** [34]. The confined MnO$_2$ are likely to exist in a more reduced state, and accordingly, the pseudocapacitive performance of MnO$_2$ can be improved by modifying the redox couples of Mn^{3+}/Mn^{4+}. The specific capacitance normalized by MnO$_2$ is almost close to the theoretical value (1250 F/g). These intriguing results may provide new insights into the configuration of MnO$_2$ with nanocarbon for developing high-performance electrode materials.
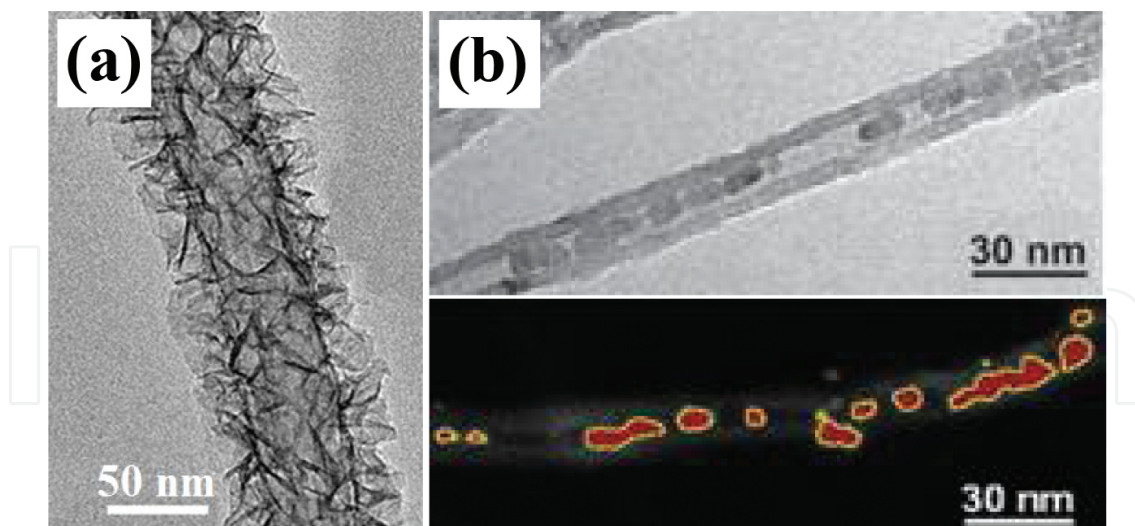
Figure 2. TEM (Transmission Electron Microscopy) images of (a) MnO$_2$-out-CNT and (b) MnO$_2$-in-CNT nanocomposites.

5.1.2. MnO$_2$-graphene

Graphene is a hottest star material in recent years due to its attractive characteristics of high electrical conductivity, good mechanical flexibility, high theoretical surface area (2600 m^2/g), and high thermal and chemical stability [35]. To exploit the potential of graphene-MnO$_2$ nanomaterials for supercapacitors, the main challenge is to prevent graphene nanosheets from restacking during material synthesis and cycling operation. MnO$_2$ nanostructures can act as interlayer spacers to effectively suppress the graphene restacking, thus facilitating fast ion diffusion/transport within the electrode materials. Moreover, the electrical intimate interaction of MnO$_2$ and graphene can boost interfacial charge transfer to ensure rapid redox reactions of MnO$_2$. In addition, graphene is capable of playing a "flexible confinement" role to enwrap MnO$_2$ nanostructures through preventing inner MnO$_2$ from electrochemical dissolution. Therefore, a strong synergetic effects benefiting from the enhanced conductivity, increased interfacial area as well as reinforced structural stability can be yielded in MnO$_2$-graphene nanocomposites. To date, a great number of studies are devoting to (i) addressing the synthesis complexity and scalability, (ii) tailoring MnO$_2$ nanostructures with a desired morphology and mass loadings in between graphene nanosheets, and (iii) improving electrical and mechanical connections between graphene and MnO$_2$.

There are two favorable approaches for the controlled fabrication of the target MnO$_2$/graphene nanocomposites. The first one is based on an *in situ* redox reaction between KMnO$_4$ and graphene or GO, as illustrated in **Figure 3a** [36]. The rich oxygen-containing functionalities of graphene layers ensure a high-MnO$_2$ mass loading. Functionalization of graphene, such as nitrogen doping, has become a key-enabling technology to improve the activities of graphene by increasing its conductivity and surface active sites. The other approach is a solution-based chemical mixing of separate MnO$_2$ nanostructures with graphene, i.e., the formation of MnO$_2$ is independent on graphene. Based on the electrostatic interaction assembly method, MnO$_2$

nanostructures can be uniformly incorporated and strong anchored in between the graphene nanosheets [22, 37]. **Figure 3b** and **c** exemplify a graphene-wrapped MnO_2 nanocomposite by co-assembling positively charged honeycomb-like MnO_2 nanospheres and negatively charged graphene nanosheets [22]. It is noted that the morphology, crystallinity, and mass loading of the nano-MnO_2 in the nanocomposites have great influence on the performance. In addition, controlling oxygen content of graphene plays a critical role in the fabrication of high-performance nanocomposites. It is believed that a simple, low-cost, and eco-friendly method is more favorable for controllably and scale-up fabricating MnO_2/graphene nanocomposites with high performance.
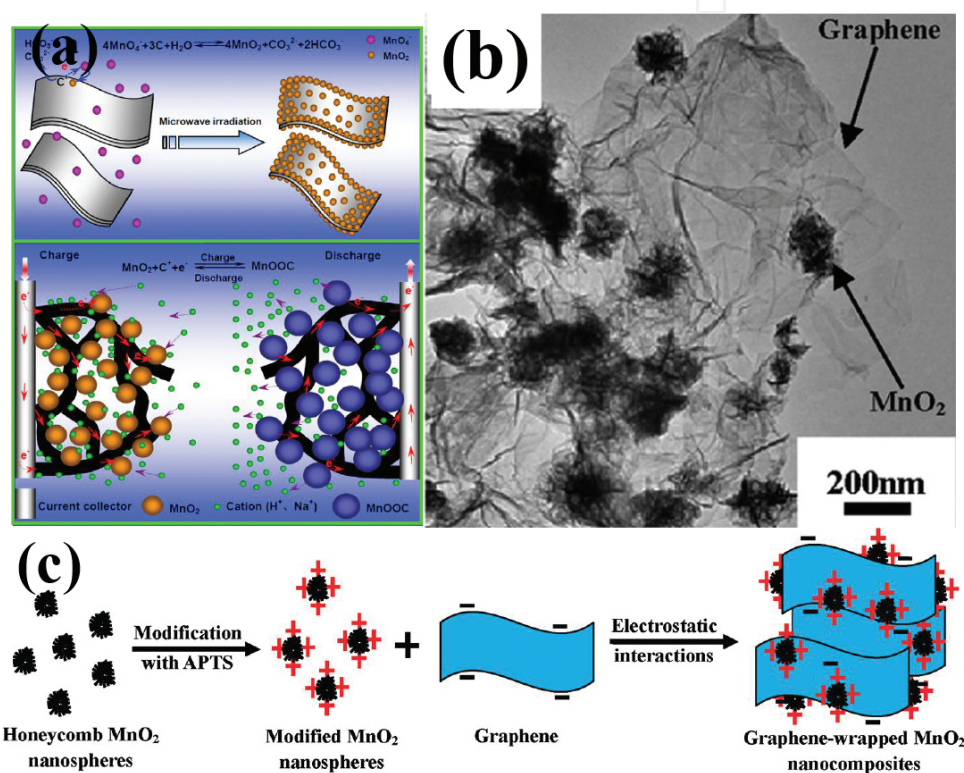

Figure 3. (a) Schematic illustration for redox deposition and charge storage process of MnO_2/graphene nanocomposite. (b) TEM image of MnO_2 honeycombs/graphene. (c) Schematic illustration for honeycomb-like MnO_2 on graphene through electrostatic assembly.

5.1.3. MnO_2/carbon nanotube/graphene

CNTs could serve as a spacer to prevent adjacent graphene nanosheets from restacking and as conductive networks to accelerate electron transport of hybrid carbon composites. Recently, a few studies have exploited MnO_2/CNT/graphene nanocomposites for high performance supercapacitors. The highly porous and conductive CNT/graphene composites can offer fast electronic and ionic channels for reversible Faradic redox reaction of MnO_2 nanostructures. MnO_2-coated CNTs were intercalated in between graphene nanosheets to form hierarchical nanocomposites [38]. The core step is the creation of positively charged MnO_2/CNT function-

alized with PDDA, which drives an electrostatical self-assembly with highly negatively charged graphene nanosheets. In this architecture, MnO_2/CNT is able to effectively prevent graphene nanosheets from severe agglomeration. In addition to solution-based chemical assembly, chemical vapor deposition (CVD) method was recently utilized to grow CNT spacers in between graphene nanosheets [39]. The highly conductive network and the porous architecture enable the nanocomposites to exhibit an improvement in the specific capacitance.

5.1.4. MnO₂-mesoporous carbon

Compared to activated carbon, ordered mesoporous carbons (OMC) possess uniform mesopores of several nanometers in diameter. The presence of the ordered mesopores is beneficial for electrolyte wetting and rapid ionic motion, which could address the rate-limiting issue of supercapacitors. The favorable mesostructure also enables OMC to be an ideal host material for compositing MnO_2 nanostructures. However, the encapsulated MnO_2 may result in disappearance of uniform mesopores and generate micropores between the nanoparticles, which prevent the mass transfer of electrolyte ions and also the formation of a double-layer required for high performance supercapacitors [40]. Hence, controlled growth of the nanoparticles homogeneously within the mesopores is crucial.
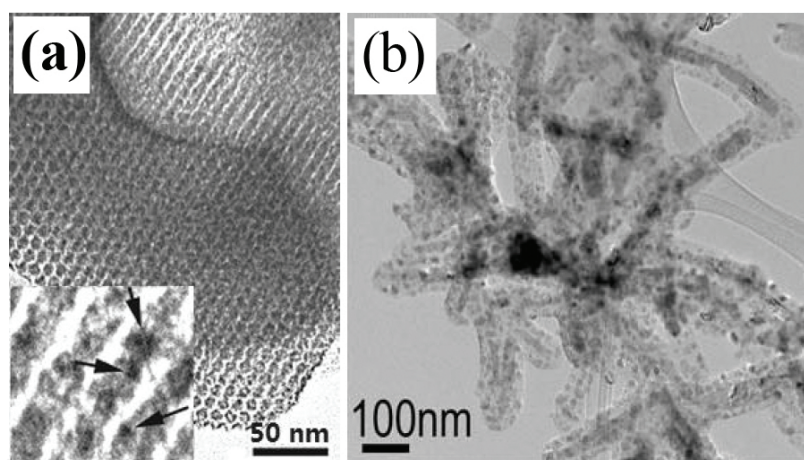

Figure 4. (a) TEM images of MnO_2/CMK-3. (b) TEM image of highly graphitic carbon-tipped MnO_x/mesoporous carbon/MnO_x hybrid nanowires.

Figure 4a exhibits a MnO_2/OMC composite prepared using an *in situ* redox reaction between $KMnO_4$ and the mesoporous carbon [41]. MnO_2 nanostructures are uniformly incorporated into the mesoporous carbon wall and the ordered mesopore structures are well-preserved. It is anticipated that OMC hosts are capable of holding the advantage of providing fast ion transport pathways for a high-rate power delivery; however, the rate capability of the composites is scarcely evaluated. This may be attributed to the relatively low electrical conductivity of OMC because the carbonization temperature is generally no more than 1000°C. This factor would become a bottle neck that would kinetically limit the charge transfer process. In combination of the favorable mesoporous structure and enhanced electrical conductivity, a

novel one-dimensional, highly graphitic carbon-tipped MnO_x/mesoporous carbon/MnO_x (MMCM) hybrid nanostructure was demonstrated as a high-performance electrode material [42]. The unique TEM image of as-prepared hybrid nanowires are illustrated in **Figure 4b**, which is different from traditional structures with MnO_2 deposited on the surfaces of carbon materials. Such a highly graphitic carbon-tipped mesoporous carbon shell provides efficient channels for ion transport into the core MnO_x and improves electrical conductivity for electron transfer. The fascinating results offer a new direction on the design of ideal electrode materials with a high-specific capacitance, an excellent rate capability, and a long-term cyclability.

5.2. MnO₂-conducting polymer nanocomposites

Conducting polymers are another class of pseudocapacitive materials due to their fast and reversible doping/undoping kinetics, ease in preparation, environmental stability, and anti-corrosion purposes [43]. The conducting polymers could provide good electronic conductivity for MnO_2, and in turn, MnO_2 offers a solid support and a percolated electrical conducting pathway by interlinking the polymer chains, thus improving charge exchange efficiency and stability during redox cycling. In combination of high pseudocapacitance of both components, a strong synergistic effect is expected to integrate into a composite of MnO_2/conducting polymers.

5.2.1. MnO₂-polyainiline (PANi)

Polyaniline (PANi) is one of the most used conducting polymers due to its high doping level, good electrical conductivity, and environmental stability. Theoretical specific capacitance of PANi reaches 750 F/g, which makes it being widely used to combine various MnO_2 [56]. $KMnO_4$ is the common oxidant to polymerize aniline monomers into PANi accompanying with an instantaneous formation of MnO_2:

$$KMnO_4 + aniline \rightarrow MnO_2 + PANi \tag{7}$$

This method leads to a good contact at an inter-molecule level between each component. It is demonstrated mesoporous MnO_2/PANi hollow spheres using an interfacial synthesis technique (**Figure 5a**) [16]. The coupling reaction was carried out at the organic/water interfacial region, favoring the self-assembly of the composites with high surface area, uniform pore-size distribution, and hierarchical architecture. In addition to the aniline monomers, PANi nanostructures were used as reactive templates to reduce $KMnO_4$, with MnO_2 nanostructures depositing onto the PANi surface. **Figure 5b** shows ultrathin MnO_2 nanorods grown on surfaces of conducting polymer nanofibers (PANi, polypyrrole (PPy), and PEDOT (poly(3,4-ethylenedioxythiophene)) by simply soaking the nanofibers in a $KMnO_4$ aqueous solution [43]. Furthermore, owing to the high chemical oxidation potential of MnO_2 (1.23 V) in an acidic condition, the aniline monomers can be polymerized with a simultaneous reduction of MnO_2 into soluble Mn^{2+} ions, which provides a rational chemical method for *in situ* dispersing MnO_2 on PANi supports [44]. Owing to the reactive template nature, morphologies of the

nanocomposites can be shaped by the pristine MnO$_2$, and the PANi content can be controlled by the polymerization time or the reaction ratio of aniline/MnO$_2$.
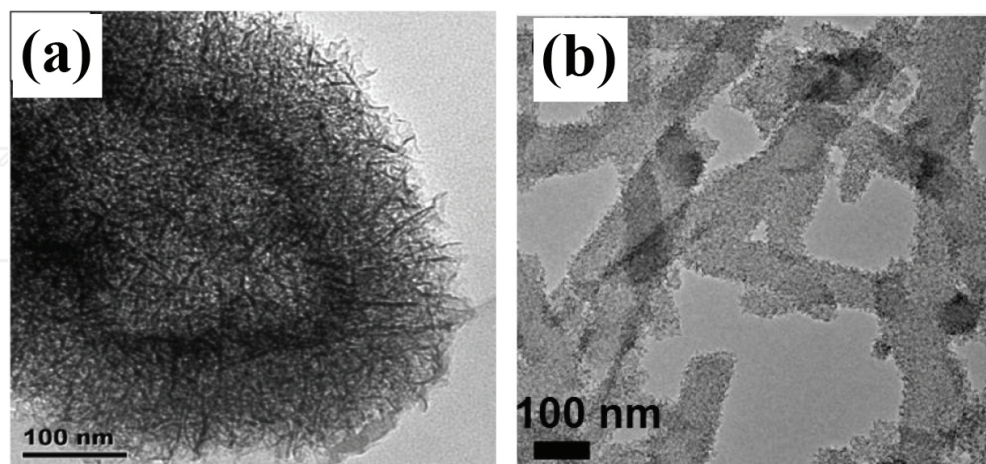

Figure 5. TEM images ofMnO$_2$/PANi (a) hollow spheres and (b) nanofibers.

5.2.2. MnO$_2$-polypyrrole (PPy)

PPy is another low-cost conducting polymer that can be used as promising electrode materials for supercapacitors. It is noteworthy that, unlike PANi showing good supercapacitive behavior in an acidic electrolyte, PPy holds the capability to possess excellent electrochemical properties in neutral electrolytes, which are highly compatible with MnO$_2$. KMnO$_4$ is a proper oxidant to chemically polymerize pyrrole monomers into PPy in relation to the formation of MnO$_2$ by reducing MnO$_4^-$ [45]. The dispersed MnO$_2$ nanoparticles adhered to PPy chains increase the surface area and retard the structural deterioration of PPy backbones. As mentioned earlier, MnO$_2$ nanostructures could serve as solid reactive templates for *in situ* polymerization of pyrrole monomers in an acidic environment, thus forming MnO$_2$/PPy nanocomposites without using any surfactants and/or additional oxidants. To this end, unique one-dimensional coaxial MnO$_2$/PPy nanotubes were developed [46, 47].

5.2.3. MnO$_2$-polythiophone (PTh)

Lu and Zhou reported a one-pot interfacial synthesis to fabricate mesoporous MnO$_2$/PTh nanocomposite having uniform submicron-sphere/nanosheet hierarchical structures [48]. The significant roles of PTh in the nanocomposite are emphasized in terms of their functions on enhancing the electrical conductivity and constraining the dissolution of MnO$_2$ component.

5.3. MnO$_2$-carbon-conducting polymer ternary nanocomposites

In order to fully exploit the advantages of different carbon and/or conducting polymers, MnO$_2$ can be combined with the dual-supports to make a maximum use of its utilization. Carbon nanostructures (e.g., CNTs) can facilitate easy electrolyte accessibility and fast electron

transport into the bulk electrode materials, meanwhile the conducting polymers can contribute to more charge storage and better inter-particle connectivity to MnO_2. This ternary design approach is expected to show improved performance, since each component in the ternary nanocomposite serves its unique and desired functions to collectively optimize their electrochemical properties.
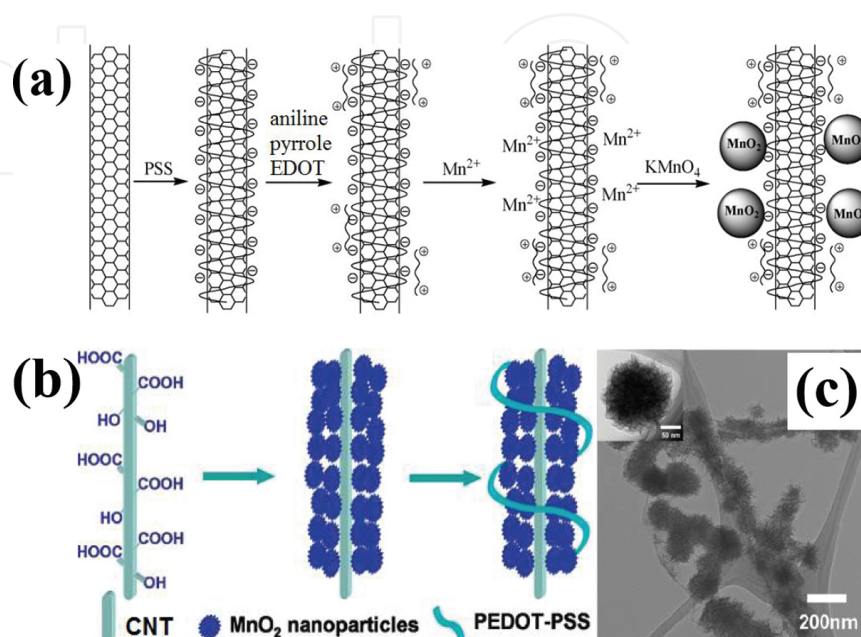

Figure 6. (a, b) Schematic illustration of synthesizing MnO_2/conducting polymers on CNTs-PSS. (c) TEM image of MnO_2/PEDOT/CNTs.

As for the MnO_2-CNT-conducting polymer nanocomposites, **Figure 6a** presents a typical synthesis route [21]. The CNT surface was modified by wrapping negatively charged PSS, which electrostatically attract Mn^{2+} species and monomers (i.e., aniline, pyrrole, and EDOT). The large number of surface sites ($-SO_3^-$) have strong interactions of growing nucleus, which facilitate an ordered growth of nanostructured MnO_2 and conducting polymers and further hinder the inter-particle agglomeration. The molecular level dispersion of MnO_2 in the CNT networks and conducting polymer matrixes results in a strong synergistic interaction. Electrochemical polymerization can also be used to deposit nanometer-thick outer layer of PEDOT onto a coaxial MnO_2/CNT composite [49]. Moreover, sonochemical processing was employed to wrap a water-soluble conducting polymer of PEDOT-PSS onto a binary composite of hierarchical MnO_2 nanospheres/CNTs, as shown in **Figure 6b** and **c** [50]. PEDOT-PSS not only served as a dispersant to stabilize the composite suspension, thus facilitating the electrode fabrication without use of binders, but also offered a good inter-particle connectivity between MnO_2 and CNTs.

5.4. Summary

Carbon nanostructures offer excellent substrates for enhancing the electrochemical performance of MnO_2. The carbon can be dispersed homogeneously into a solution, facilitating a

uniform deposition of MnO$_2$ nanodeposits onto the carbon surface through a solution-based processing. The high surface area of carbon supports also provides a large number of anchoring sites for MnO$_2$ formation and enlarges the contact interfaces between MnO$_2$ and electrolyte. It is worthy to note that a porous carbon having well-ordered pore channels can permit fast electrolyte transport, meanwhile, a well-graphitic carbon with enhanced electrical conductivity can enable rapid charge collection/transfer under a high-rate operation. Conducting polymers can work in good synergy with MnO$_2$ to capture a maximum electrochemical harvesting from the large pseudocapacitances. A rational design strategy is necessary to control the MnO$_2$ dispersion into conducting polymers by tuning the synthesis conditions. For the *in situ* redox deposition, the mass loading of MnO$_2$ is extremely limited because an over-oxidation of conducting polymers would destroy their π-conjugated structure, and accordingly, substantially lose their conductivities and electroactivities. A better synthesis alternative is to use MnO$_2$ nanostructures as reactive templates for polymerizing polymer monomers surrounding its outmost surfaces. The synchronous formation of MnO$_2$ and conducting polymers in the chemical co-precipitation method facilitates a molecular level interaction with each other, but the electrochemical performance depends on the morphologies of the nano-composites. Interfacial synthesis is an optional approach to prepare a composite with meso-porous structure.

Ternary nanocomposites are capable of maximizing the desirable functions of each component. The synergistic contribution results in great capacitance enhancement, high-rate delivery and better cycling performance. Furthermore, it is important to bridge MnO$_2$ and carbon to electrolytes with a large interaction area by controlling the thickness of conducting polymer layers and their spatial distribution in the ternary structure.

6. Asymmetric supercapacitors based on MnO$_2$ nanostructures

6.1. Fabrication principles

To make an asymmetric supercapacitor that can operated stably in a wide potential range, the critical issue is to couple electrode materials with different high overpotentials for hydrogen or oxygen evolutions [51]. It is known that MnO$_2$ nanostructures normally work in the electrochemical potential window of 0.0–1.0 V (vs. SCE). Therefore, the coupled electrode materials should have a potential window in a range far beyond 0.0–1.0 V. Since the first report of MnO$_2$|| activated carbon asymmetric supercapacitor by Hong et al. in 2002 [52], carbon materials have attracted massive attention as coupled electrodes, because they can operate in a wide potential window from −1.0 to 0.1 V vs. SCE (Saturated Calomel Electrode) [17]. A wide operating potential window of 2.0 V is yielded in the assembled asymmetric supercapacitor in a Na$_2$SO$_4$ aqueous electrolyte. The asymmetric supercapacitor could even work in a working voltage as high as 2.3 V after elaborating the electrode materials (e.g., mass ratio) and cell assembly (e.g., oxygen expelling). Such a high-cell voltage is comparable to a commercially available symmetric supercapacitors using organic electrolyte (2.5 V) [51]. Consequently, the energy density of asymmetric supercapacitors is exceptionally high, reaching over 20 Wh/kg,

almost one order of magnitude higher than that of the aqueous-based symmetric supercapacitor and also greater than that of organic-based SSCs (17–18 Wh/kg).

In addition to the carbon materials, pseudocapacitive materials, such as metal oxides and conducting polymers (e.g., PANi, PPy, and PEDOT), can be used as coupled electrodes for asymmetric supercapacitors. It is noted that the electrochemical oxidation/reduction potential is essentially associated with the work function of a metal oxide [53]. A large work function difference of two metal oxides provide an opportunity of enlarging operating voltage larger than the dissociation energy of an aqueous electrolyte because the water decomposition is kinetically limited by hydrogen and oxygen evolution reaction on the surface of metal oxides. Hence, a metal oxide with a largest work function difference from MnO_2 is more appropriate for asymmetric supercapacitor assembly to maximizing cell voltage in neutral aqueous electrolytes.

Moreover, another important technological issue is to balance the charge (Q) that stored at positive and negative electrodes. The charge stored by each electrode is linearly proportional to the specific capacitance (C), the potential window (ΔU), and the mass (m) of an electrode material, i.e., $Q = C \times \Delta U \times m$. In order to obtain charge balance, i.e., $Q_+ = Q_-$, the optimal mass ratio of the positive electrode (m_+) against negative electrode (m_-) can be estimated according to Eq. (8) [17]. It should be noted that the optimal mass ratio is responsible for an ideal capacitive behavior with a maximum cell voltage and a high-Coulombic efficiency.

$$\frac{m_+}{m_-} = \frac{C_- \times \Delta U_-}{C_+ \times \Delta U_+} \tag{8}$$

6.2. Asymmetric supercapacitor cells

Carbon materials are of particular interest as negative electrodes for asymmetric supercapacitors due to their characteristics of good EDLC, a high-overpotential for hydrogen evolution, excellent electrical conductivity for high power delivery, and good chemical inertness for long cycle life. In this regard, various carbon materials have been explored including graphene, CNTs, activated carbon nanofibers (ACNFs), carbon sphere (CS), ordered mesoporous carbon, etc., to couple MnO_2.

Graphene-based materials have been received intensive attention for asymmetric supercapacitors. First, graphene itself exhibits outstanding physiochemical and capacitive properties. Second, the ultrathin two-dimensional structure of graphene provides a large surface area for anchoring MnO_2 nanostructures [54, 55]. In addition, graphene-based materials can also be compacted into free-standing electrodes, which endow asymmetric supercapacitor with flexibility and lightweight. The energy and power values would be more fascinating at a device level taking the additives (binders and conductors) and the current collectors into account. **Figure 7** demonstrated porous hybrid thin-film structures of MnO_2/graphene and graphene/Ag, which are highly flexible, mechanically robust, and ultra-lightweight using the ordinal filtration assembly method [55]. The flexible device extended the operating potential window to 1.8 V and showed an energy density of 50.8 Wh/kg.
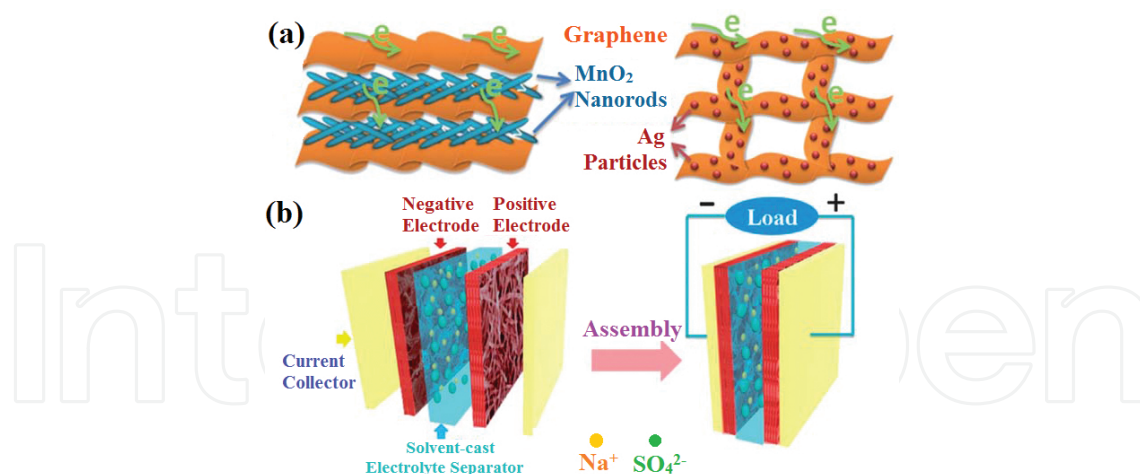
Figure 7. Illustrations of (a) MnO₂/graphene and graphene/Ag freestanding films and (b) the as-fabricated asymmetric supercapacitor devices.

CNTs and carbon nanofiber fabrics were demonstrated to serve excellent one-dimensional negative materials for energy storage devices due to their high electrical conductivity, good mechanical stability, and flexibility [56–60]. On one hand, MnO_2 nanostructures can be uniformly deposited surround the one-dimensional carbons and the resulting nanocomposites showed pronounced electrochemical properties. On the other hand, the porous one-dimensional carbons possess good electric double-layer capacitance, thus becoming highly promising negative candidates for asymmetric supercapacitors. The asymmetric supercapacitors assembled by one-dimensional carbons as the negative electrodes and MnO_2/carbon nanocomposites as the positive electrode can be cycled reversibly in a high-voltage region of 0–2.0 V and exhibited a superior energy density of 30–35 Wh/kg in a neutral aqueous Na_2SO_4 electrolyte. In particular, the asymmetric supercapacitors based on electrospun carbon nanofibers are rather promising to meet the ever-increasing demands of high energy/power densities because of the scalability, easy-fabrication, and low-cost of the electrospinning technique [56].

In addition to the carbon materials, metal oxides and conducting polymers, such as SnO_2, MoO_3 PANi, PPy, and PEDOT, were also explored as negative materials to couple MnO_2 nanostructures [51, 61]. MoO_3 would be the most favorable coupled pair of MnO_2 because of their largest work function difference [53]. To this end, MoO_3/graphene composite and MnO_2/graphene nanocomposite were prepared to serve as the negative electrode and the positive electrode for the fabrication of an asymmetric supercapacitor. The as-assembled device can operated stably in a wide voltage window of 2.0 V, and more significantly, exhibited a high-specific capacitance of 307 F/g and a high-energy density of 42.6 Wh/kg.

7. Summaries and perspectives

MnO₂-based electrode materials hold a particular prospect for future supercapacitor applications although there are still some obstacles that need to be conquered. To better utilize the

electrochemical performance of MnO_2, it is necessary to create more electrochemically active sites or reduce the ion/electron transport distance by modifying surface chemistry and structure of MnO_2. One of the most effective approaches is incorporating nanoscaled MnO_2 into a highly porous and electronically conductive framework, such as carbon scaffolds and conducting polymers, to form a hybrid material. Benefiting from the synergistic contribution from each component in the composite, the consistent progress in the research and development of MnO_2-based nanocomposites have achieved many breakthroughs in terms of charge storage mechanism, smart design strategies, and technological innovations. It should be noted that more advanced characterization tools and new methodologies as well systematic studies are still required to deepen the fundamental understanding of material chemistry and electrode/electrolyte interface. The energy and power densities of supercapacitors can be significantly improved by one magnitude through a simple asymmetric configuration method. Although many limiting factors, such as optimal coupled electrode, high-cost issue, complex fabrication process, moderate cycle life, etc., are required to be conquered urgently, it is believed that the ongoing research would bring MnO_2-based asymmetric supercapacitors to an acceptable level for practical applications.

Acknowledgements

Author details

Jian-Gan Wang

Address all correspondence to: wangjiangan@nwpu.edu.cn

State Key Laboratory of Solidification Processing, Center for Nano Energy Materials, School of Materials Science and Engineering, Northwestern Polytechnical University, Xi'an, China

References

[1] Salanne M, Rotenberg B, Naoi K, Kaneko K, Taberna PL, Grey CP, Dunn B, Simon P. Efficient storage mechanisms for building better supercapacitors. Nature Energy. 2016; 1: 16070. doi:10.1038/NENERGY.2016.70

[2] Lee HY, Goodenough JB. Supercapacitor behavior with KCl electrolyte. Journal of Solid State Chemistry. 1999; 144: 220–223. doi:10.1006/jssc.1998.8128

[3] Toupin M, Brousse T, Bélanger D. Charge storage mechanism of MnO₂ electrode used in aqueous electrochemical capacitor. Chemistry of Materials. 2004; 16: 3184–3190. doi:10.1021/cm049649j

[4] Wei W, Cui X, Chen W, Ivey DG. Manganese oxide-based materials as electrochemical supercapacitor electrodes. Chemical Society Reviews. 2011; 40: 1697–1721. doi:10.1039/C0CS00127A

[5] Xu C, Kang F, Li B, Du H. Recent progress on manganese dioxide based supercapacitors. Journal of Materials Research. 2010; 25: 1421–1432. doi:10.1557/JMR.2010.0211

[6] Zhai T, Lu X, Wang F, Xia H, Tong Y. MnO₂ nanomaterials for flexible supercapacitors: performance enhancement via intrinsically and extrinsically modification. Nanoscale Horizons. 2016; 1: 109–124. doi:10.1039/c1035nh00048c.

[7] Ghodbane O, Pascal JL, Favier F. Microstructural effects on charge-storage properties in MnO₂-based electrochemical supercapacitors. ACS Applied Materials and Interfaces. 2009; 1: 1130–1139. doi:10.1021/am900094e

[8] Ghodbane O, Pascal JL, Fraisse B, Favier F. Structural *in situ* study of the thermal behavior of manganese dioxide materials: toward selected electrode materials for supercapacitors. ACS Applied Materials and Interfaces. 2010; 2: 3493–3505. doi:10.1021/am100669k

[9] Kuo SL, Wu NL. Investigation of pseudocapacitive charge-storage reaction of MnO₂° nH₂O supercapacitors in aqueous electrolytes. Journal of The Electrochemical Society. 2006; 153: A1317–A1324. doi:10.1149/1.2197667

[10] Ghaemi M, Ataherian F, Zolfaghari A, Jafari S. Charge storage mechanism of sono-chemically prepared MnO₂ as supercapacitor electrode: effects of physisorbed water and proton conduction. Electrochimica Acta. 2008; 53: 4607–4614. doi:10.1016/j.electacta.2007.12.040

[11] Brousse T, Toupin M, Dugas R, Athouël L, Crosnier O, Bélanger D. Crystalline MnO₂ as possible alternatives to amorphous compounds in electrochemical supercapacitors. Journal of The Electrochemical Society. 2006; 153: A2171–A2180. doi:10.1149/1.2352197

[12] Devaraj S, Munichandraiah N. Effect of crystallographic structure of MnO₂ on its electrochemical capacitance properties. The Journal of Physical Chemistry C. 2008; 112: 4406–4417. doi:10.1021/jp7108785

[13] Chang JK, Lee MT, Tsai WT, Deng MJ, Sun IW. X-ray photoelectron spectroscopy and *in situ* X-ray absorption spectroscopy studies on reversible insertion/desertion of dicyanamide anions into/from manganese oxide in ionic liquid. Chemistry of Materials. 2009; 21: 2688–2695. doi:10.1021/cm9000569

[14] Song MK, Cheng S, Chen H, Qin W, Nam KW, Xu S, Yang XQ, Bongiorno A, Lee J, Bai J. Anomalous pseudocapacitive behavior of a nanostructured, mixed-valent manganese oxide film for electrical energy storage. Nano Letters. 2012; 12: 3483–3490. doi: 10.1021/nl300984y

[15] Wang JG, Yang Y, Huang ZH, Kang F. Shape-controlled synthesis of hierarchical hollow urchin-shape α-MnO_2 nanostructures and their electrochemical properties. Materials Chemistry and Physics. 2013; 140: 643–650. doi:10.1016/j.matchemphys.2013.04.018

[16] Wang JG, Yang Y, Huang ZH, Kang F. Interfacial synthesis of mesoporous MnO_2/polyaniline hollow spheres and their application in electrochemical capacitors. Journal of Power Sources. 2012; 204: 236–243. doi:10.1016/j.jpowsour.2011.12.057

[17] Wang JG, Kang F, Wei B. Engineerging of MnO_2-based nanocomposites for high performance supercapacitors. Progress in Materials Science. 2015; 74: 51–124. doi: 10.1016/j.pmatsci.2015.04.003

[18] Zhang H, Cao G, Wang Z, Yang Y, Shi Z, Gu Z. Growth of manganese oxide nanoflowers on vertically-aligned carbon nanotube arrays for high-rate electrochemical capacitive energy storage. Nano Letters. 2008; 8: 2664–2668. doi:10.1021/nl800925j

[19] Liu R, Lee SB. MnO_2/poly (3, 4-ethylenedioxythiophene) coaxial nanowires by one-step coelectrodeposition for electrochemical energy storage. Journal of the American Chemical Society. 2008; 130: 2942–2943. doi:10.1021/ja7112382

[20] Liu J, Essner J, Li J. Hybrid supercapacitor based on coaxially coated manganese oxide on vertically aligned carbon nanofiber arrays. Chemistry of Materials. 2010; 22: 5022–5030. doi:10.1021/cm101591p

[21] Sharma RK, Zhai L. Multiwall carbon nanotube supported poly (3, 4-ethylenedioxythiophene)/manganese oxide nano-composite electrode for super-capacitors. Electrochimica Acta. 2009; 54: 7148–7155. doi:10.1016/j.electacta.2009.07.048

[22] Zhu J, He J. Facile synthesis of graphene-wrapped honeycomb MnO_2 nanospheres and their application in supercapacitors. ACS Applied Materials and Interfaces. 2012; 4: 1770–1776. doi:10.1021/am3000165

[23] Wang JG, Yang Y, Huang ZH, Kang F. Effect of Fe^{3+} on the synthesis and electrochemical performance of nanostructured MnO_2. Materials Chemistry and Physics. 2012; 133: 437–444. doi:10.1016/j.matchemphys.2012.01.056

[24] Ragupathy P, Park DH, Campet G, Vasan HN, Hwang SJ, Choy JH, Munichandraiah N. Remarkable capacity retention of nanostructured manganese oxide upon cycling as an electrode material for supercapacitor. The Journal of Physical Chemistry C. 2009; 113: 6303–6309. doi:10.1021/jp811407q

[25] Hu CC, Wang CC. Nanostructures and capacitive characteristics of hydrous manganese oxide prepared by electrochemical deposition. Journal of The Electrochemical Society. 2003; 150: A1079–A1084. doi:10.1149/1.1587725

[26] Wei W, Cui X, Mao X, Chen W, Ivey DG. Morphology evolution in anodically electro-deposited manganese oxide nanostructures for electrochemical supercapacitor applications—effect of supersaturation ratio. Electrochimica Acta. 2011; 56: 1619–1628. doi:10.1016/j.electacta.2010.10.044

[27] Xu CL, Bao SJ, Kong LB, Li H, Li HL. Highly ordered MnO$_2$ nanowire array thin films on Ti/Si substrate as an electrode for electrochemical capacitor. Journal of Solid State Chemisitry. 2006; 179: 1351–1355. doi:10.1016/j.jssc.2006.01.058

[28] Wei J, Zhitomirsky I. Electrosynthesis of manganese oxide films. Surface Engineering. 2008; 24: 40–46. doi:10.1179/174329408X271363

[29] Yuan C, Gao B, Shen L, Yang S, Hao L, Lu X, Zhang F, Zhang L, Zhang X. Hierarchically structured carbon-based composites: design, synthesis and their application in electrochemical capacitors. Nanoscale. 2011; 3: 529–545. doi:10.1039/C0NR00423E

[30] Zhang LL, Zhao XS. Carbon-based materials as supercapacitor electrodes. Chemical Society Reviews. 2009; 38: 2520–2531. doi:10.1039/B813846J

[31] Wang JG, Yang Y, Huang ZH, Kang F. Coaxial carbon nanofibers/MnO$_2$ nanocomposites as freestanding electrodes for high-performance electrochemical capacitors. Electro-chimica Acta. 2011; 56: 9240–9247. doi:10.1016/j.electacta.2011.07.140

[32] Wang JG, Yang Y, Huang ZH, Kang F. Synthesis and electrochemical performance of MnO$_2$/CNTs–embedded carbon nanofibers nanocomposites for supercapacitors. Electrochimica Acta. 2012; 75:213–219. doi:10.1016/j.electacta.2012.04.088

[33] Xia H, Wang Y, Lin J, Lu L. Hydrothermal synthesis of MnO$_2$/CNT nanocomposite with a CNT core/porous MnO$_2$ sheath hierarchy architecture for supercapacitors. Nanoscale Research Letters. 2012; 7: 1–10. doi:10.1186/1556-276X-7-33

[34] Chen W, Fan Z, Gu L, Bao X, Wang C. Enhanced capacitance of manganese oxide via confinement inside carbon nanotubes. Chemical Communications. 2010; 46: 3905–3907. doi:10.1039/c000517g

[35] Shao Y, El-Kady MF, Wang LJ, Zhang Q, Li Y, Wang H, Mousavi MF, Kaner RB. Graphene-based materials for flexible supercapacitors. Chemical Society Reviews. 2015; 44: 3639–3665. doi:10.1039/c4cs00316k

[36] Yan J, Fan Z, Wei T, Qian W, Zhang M, Wei F. Fast and reversible surface redox reaction of graphene–MnO$_2$ composites as supercapacitor electrodes. Carbon. 2010; 48: 3825–3833. doi:10.1016/j.carbon.2010.06.047

[37] Chen S, Zhu J, Wu X, Han Q, Wang X. Graphene oxide–MnO$_2$ nanocomposites for supercapacitors. ACS Nano. 2010; 4: 2822–2830. doi:10.1021/nn901311t

[38] Lei Z, Shi F, Lu L. Incorporation of MnO$_2$-coated carbon nanotubes between graphene sheets as supercapacitor electrode. ACS Applied Materials and Interfaces. 2012; 4: 1058–1064. doi:10.1021/am2016848

[39] Jiang H, Dai Y, Hu Y, Chen W, Li C. Nanostructured ternary nanocomposite of rGO/CNTs/MnO$_2$ for high-rate supercapacitors. ACS Sustainable Chemistry and Engineering. 2013; 2: 70–74. doi:10.1021/sc400313y

[40] Jiang H, Ma J, Li C. Mesoporous carbon incorporated metal oxide nanomaterials as supercapacitor electrodes. Advanced Materials. 2012; 24: 4197–4202. doi:10.1002/adma.201104942

[41] Dong X, Shen W, Gu J, Xiong L, Zhu Y, Li H, Shi J. MnO$_2$-embedded-in-mesoporous-carbon-wall structure for use as electrochemical capacitors. The Journal of Physical Chemistry B. 2006; 110: 6015–6019. doi:10.1021/jp056754n

[42] Jiang H, Yang L, Li C, Yan C, Lee PS, Ma J. High-rate electrochemical capacitors from highly graphitic carbon–tipped manganese oxide/mesoporous carbon/manganese oxide hybrid nanowires. Energy and Environmental Science. 2011; 4: 1813–1819. doi:10.1039/c1ee01032h

[43] Han J, Li L, Fang P, Guo R. Ultrathin MnO$_2$ nanorods on conducting polymer nanofibers as a new class of hierarchical nanostructures for high-performance supercapacitors. The Journal of Physical Chemistry C. 2012; 116: 15900–15907. doi:10.1021/jp303324x

[44] Jafri RI, Mishra AK, Ramaprabhu S. Polyaniline–MnO$_2$ nanotube hybrid nanocomposite as supercapacitor electrode material in acidic electrolyte. Journal of Materials Chemistry. 2011; 21: 17601–17605. doi:10.1039/c1jm13191e

[45] Zang J, Li X. *In situ* synthesis of ultrafine β-MnO$_2$/polypyrrole nanorod composites for high-performance supercapacitors. Journal of Materials Chemistry. 2011; 21: 10965–10969. doi:10.1039/c1jm11491c

[46] Wang JG, Yang Y, Huang ZH, Kang F. MnO$_2$/polypyrrole nanotubular composites: reactive template synthesis, characterization and application as superior electrode materials for high-performance supercapacitors. Electrochimica Acta. 2014; 130: 642–649. doi:10.1016/j.electacta.2014.03.082

[47] Wang JG, Yang Y, Huang ZH, Kang F. Facile synthesis of hierarchical conducting polypyrrole nanostructures via a reactive template of MnO$_2$ and their application in supercapacitors. RSC Advances. 2014; 4: 199–202. doi:10.1039/c3ra45824e

[48] Lu Q, Zhou Y. Synthesis of mesoporous polythiophene/MnO$_2$ nanocomposite and its enhanced pseudocapacitive properties. Journal of Power Sources. 2011; 196: 4088–4094. doi:10.1016/j.jpowsour.2010.12.059

[49] Yoon SB, Kim KB. Effect of poly (3, 4-ethylenedioxythiophene)(PEDOT) on the pseudocapacitive properties of manganese oxide (MnO$_2$) in the PEDOT/MnO$_2$/multiwall carbon nanotube (MWNT) composite. Electrochimica Acta. 2013: 106: 135–142. doi:10.1016/j.electacta.2013.05.058

[50] Hou Y, Cheng Y, Hobson T, Liu J. Design and synthesis of hierarchical MnO$_2$ nanospheres/carbon nanotubes/conducting polymer ternary composite for high perform-

ance electrochemical electrodes. Nano Letters. 2010; 10: 2727–2733. doi:10.1021/nl101723g

[51] Zhang J, Zhao XS. On the configuration of supercapacitors for maximizing electrochemical performance. ChemSusChem. 2012; 5: 818–841. doi:10.1002/cssc.201100571

[52] Hong MS, Lee SH, Kim SW. Use of KCl aqueous electrolyte for 2 V manganese oxide/activated carbon hybrid capacitor. Electrochemical Soild-State Letters. 2002; 5: A227–A230. doi:10.1149/1.1506463

[53] Chang J, Jin M, Yao F, Kim TH, Le VT, Yue H, Gunes F, Li B, Ghosh A, Xie S, Lee YH. Asymmetric supercapacitors based on graphene/MnO₂ nanospheres and graphene/MoO₃ nanosheets with high energy density. Advanced Functional Materials. 2013; 23: 5074–5083. doi:10.1002/adfm201301851

[54] Wu ZS, RenW, Wang DW, Li F, Liu B, Cheng HM. High-energy MnO₂ nanowire/graphene and graphene asymmetric electrochemical capacitors. ACS Nano. 2010; 4: 5835–5842. doi:10.1021/nn101754k

[55] Shao Y, Wang H, Zhang Q, Li Y. High-performance flexible asymmetric supercapacitors based on 3D porous graphene/MnO₂ nanorod and graphene/Ag hybrid thin-film electrodes. Journal of Materials Chemistry C. 2013; 1: 1245–1251. doi:10.1039/c2tc00235c

[56] Wang JG, Yang Y, Huang ZH, Kang F. A high-performance asymmetric supercapacitor based on carbon and carbon-MnO₂ nanofiber electrodes. Carbon. 2013; 61:190–199. doi:10.1016/j.carbon.2013.04.084

[57] Yu G, Hu L, Vosgueritchian M, Wang H, Xie X, McDonough JR, Cui X, Cui Y, Bao Z. Solution-processed graphene/MnO₂ nanostructured textiles for high-performance electrochemical capacitors. Nano Letters. 2011; 11: 2905–2911. doi:10.1021/nl2013828

[58] Wang JG, Yang Y, Huang ZH, Kang F. Incorporation of nanostructured manganese dioxide into carbon nanofibers and its electrochemical performance. Materials Letters. 2012; 72: 18–21. doi:10.1016/j.matlet.2011.12.071

[59] Wang JG, Yang Y, Huang ZH, Kang F. Rational synthesis of MnO₂/conducting polypyrrole@carbon nanofiber triaxial nano-cables for high-performance supercapacitors. Journal of Materials Chemistry. 2012; 22: 16943–16949. doi:10.1039/c2jm33364c

[60] Wang JG, Yang Y, Huang ZH, Kang F. Effect of temperature on the pseudo-capacitive behavior of freestanding MnO₂@ carbon nanofibers composites electrodes in mild electrolyte. Journal of Power Sources. 2013; 224: 86–92. doi:0.1016/j.jpowsour.2012.09.075

[61] Ng KC, Zhang S, Chen GZ. An asymmetrical supercapacitor based on CNTs/SnO₂ and CNTs/MnO₂ nanocomposites working at 1.7 V in aqueous electrolyte. ECS Transactions. 2008; 16: 153–162. doi:10.1149/1.2985638